



Cite this: *RSC Adv.*, 2022, 12, 31246

# Flexible selection of the functional-group ratio on a polytetrafluoroethylene (PTFE) surface using a single-gas plasma treatment†

Yuji Ohkubo, \* Yuki Okazaki, Misa Nishino, Yosuke Seto, Katsuyoshi Endo and Kazuya Yamamura

During plasma treatment of polymers, etching occurs and functional groups are introduced on their surface. We assumed that controlling the etching rate would enable plasma treatment using a single gas to control the ratio of functional groups generated on a polymer's surface, although previous studies have indicated that several different types of functional groups are formed when the gaseous species are varied. In this study, we selected the base pressure (BP) as a parameter for controlling the etching rate and subjected polytetrafluoroethylene (PTFE) to plasma treatments using only He gas at various BPs. The chemical composition of the surface of the plasma-treated PTFE samples was evaluated by X-ray photoelectron spectroscopy (XPS), and the ratios of fluorine (CF<sub>3</sub>, CF<sub>2</sub>, C–F), oxygen (O–C=O, C=O, C–O), and carbon (C–C, C=C) groups were quantified from the C 1s-XPS spectra. The fluorine-group ratio decreased and the oxygen- and carbon-group ratios increased with decreasing BP. The results demonstrated that plasma treatment using a single gas enabled flexible selection of the ratio of functional groups generated on PTFE via control of the BP.

Received 30th July 2022  
Accepted 21st October 2022

DOI: 10.1039/d2ra04763b

rsc.li/rsc-advances

## Introduction

Polytetrafluoroethylene (PTFE) is a fluoropolymer consisting of only C and F atoms. It exhibits numerous excellent properties, including good performance as a high-frequency material, high water and oil repellency, good chemical resistance, high thermal resistance, and a low coefficient of friction. Therefore, PTFE has been used as an electret material,<sup>1</sup> super-hydrophobic material,<sup>2</sup> and protection material<sup>3</sup> *etc.* in various fields recently. However, PTFE has the disadvantage of exhibiting poor adhesion because of its low surface energy and the presence of a low-molecular-weight layer known as a weak boundary layer (WBL).<sup>4–7</sup> These shortcomings limit the range of application of PTFE, necessitating improvements in its adhesion properties through the modification of its surface.

Chemical etching treatments using a Na-naphthalene or Na-ammonium complex solution are widely used to improve the adhesion properties of PTFE. This process greatly improves the adhesion properties of PTFE because the WBL is removed and O-containing functional groups are introduced by surface etching due to the strong reducing power of Na. However, this process has numerous problems in that the etching dramatically increases the surface roughness, Na-containing solutions

are hazardous to humans and the environment, and the treatment discolors the surface of PTFE.<sup>6,8–12</sup> These shortcomings have led researchers to investigate plasma treatment as an ecofriendly surface-modification method.

In previous studies involving plasma treatment of polymers, plasma treatment was performed as various parameters such as the gaseous species, plasma treatment times, gas flow rates, and input power were varied. Regarding the gaseous species, plasma treatments for various polymers such as PTFE, tetrafluoroethylene and perfluoroalkoxyvinyl ether copolymer (PFA), polyvinyl fluoride (PVF), polyvinylidene difluoride (PVDF), polyethylene (PE), polyethylene terephthalate (PET), and polystyrene (PS), polyamide (PA), polyimide (PI) using He,<sup>13–15</sup> Ar,<sup>11,13,16–19</sup> O<sub>2</sub>,<sup>11,13,18</sup> H<sub>2</sub>,<sup>13,20,21</sup> hydrogen sulfide (H<sub>2</sub>S),<sup>22</sup> carbon tetrafluoride (CF<sub>4</sub>),<sup>13</sup> NH<sub>3</sub>,<sup>23</sup> He + O<sub>2</sub>,<sup>15,24</sup> Ar + O<sub>2</sub>,<sup>17</sup> N<sub>2</sub> + H<sub>2</sub>,<sup>25,26</sup> N<sub>2</sub> + NH<sub>3</sub>,<sup>25,27</sup> H<sub>2</sub> + sulfur dioxide (SO<sub>2</sub>),<sup>20</sup> Ar + acrylic acid,<sup>28–30</sup> and Ar + NH<sub>3</sub> + H<sub>2</sub>O (ref. 31) have been reported. Plasma treatment using a noble gas such as He or Ar is safe and can promote both the desorption of F on the surface of PTFE, PFA, and PVF and C–C crosslinking.<sup>11,13,15–17</sup> Subsequent air exposure can introduce O-containing functional groups such as C=O and C–O.<sup>16</sup> Plasma treatment using O<sub>2</sub> or He + O<sub>2</sub> or Ar + O<sub>2</sub> gas was found to have the greatest effect on the etching rate and to introduce few functional groups onto the surface.<sup>11,15,17,24</sup> Plasma treatment using H<sub>2</sub> gas was found to promote the desorption of F on the surface and to introduce functional groups such as C–O and C–C (C–H).<sup>13,20,21</sup> Plasma treatment using H<sub>2</sub>S or H<sub>2</sub> + SO<sub>2</sub> introduced a large number of thiol groups (S–H) onto the PTFE

Graduate School of Engineering, Osaka University, 2-1 Yamadaoka, Suita, Osaka 565-0871, Japan. E-mail: okubo@upst.eng.osaka-u.ac.jp

† Electronic supplementary information (ESI) available. See DOI: <https://doi.org/10.1039/d2ra04763b>



surface and formed a S-containing film on the surface.<sup>20,22</sup> Plasma treatment using  $N_2 + H_2$  or  $N_2 + NH_3$  introduced functional groups such as C–N (C–O) and C–C (C–H) to the surface of PTFE and PVDF.<sup>25,26</sup> The number of functional groups introduced onto the PTFE and PVDF surface plasma-treated using  $N_2 + NH_3$  was greater than that introduced onto the PTFE surface plasma-treated using  $N_2 + H_2$ .  $NH_3$  gas has a pungent odor and is toxic and must therefore be used carefully. Plasma treatment using acrylic acid was found to introduce functional groups such as O–C=O, –C=O, –C–O–, and C–C (C–H).<sup>28–30</sup> In these studies, the acrylic-acid-plasma-polymerized PTFE/epoxy (EP)-adhesive/Al adhesion strength was evaluated and found to be 70 times greater than the adhesion strength of as-received PTFE. However, acrylic acid gas is inflammable and explosive. In  $CF_4$  plasma,  $CF_3$ ,  $CF_2$ , and C–F radicals were generated and both surface planarization and hydrophobization of the PTFE surface were promoted.<sup>13</sup> Regarding the plasma treatment time and gas flow rate, the surface conditions did not change when the plasma treatment time and gas flow rate were increased above a certain value.<sup>11,15</sup> Also, regarding the input power for plasma generation, the ratio of O-containing functional groups, surface hardness, and adhesion strength increased with increasing input power.<sup>32</sup> As previously discussed, most of the previous related reports have focused on functional-group formation, whereas few reports have focused on etching. Etching on a PTFE surface plays an important role in breaking C–F and C–C bonds and in removing the WBL from the PTFE surface. Except for Inagaki's report on the etching rate on a PET surface,<sup>33</sup> Prime's review report that O-containing functional groups on the PTFE surface was inversely dependent on the concentration of oxygen in plasma treatment,<sup>34</sup> and Ohkubo's report that the influence of air contamination during heat-assisted plasma (HAP) treatment,<sup>35</sup> the literature contains few discussions about etching rates. They suggested that the etching depended on the oxygen concentration in the plasma treatment and that the etching effect correlated with the condition of the plasma-treated surface. However, the question of whether the surface is excessively etched or the plasma-modified layer is also etched has not been investigated. Therefore, an investigation of the relation between the etching rate and the surface condition is needed. Also, in previous reports,<sup>13,20,31</sup> plasma gaseous species were varied to change the type of functional group formed on the surface and to control the ratios of the functional groups. However, to the best of our knowledge, the literature contains no studies in which a plasma treatment involving a single gas was used to vary the ratio of functional groups. If the etching rate can be controlled and inhibit excessive etching of the plasma-modified layer, it may be possible to retain O-containing functional groups and C–C crosslinkings on the PTFE surface, enabling the ratio of functional groups formed on the surface to be controlled. We hypothesized that controlling the etching rate by manipulating the base pressure (BP) would inhibit excessive etching of the PTFE surface and enable control of the ratio of functional groups even with a single gas. In this work, we investigated the relations among the BP, etching rate, surface chemical composition, surface morphology, surface hardness, and

adhesion properties of PTFE to verify this hypothesis. Additionally, we aimed to realize a flexible selection from PTFE surfaces having different functional-group ratios according to the application.

## Experimental

### Materials

PTFE sheets (NITOFLOX No. 900UL, Nitto Denko, Japan) were cut to dimensions of  $L = 70$  mm,  $W = 45$  mm,  $t = 0.2$  mm and used as fluoropolymer samples. The cut PTFE sheets were washed with acetone (99.5%, Kishida Chemical, Japan) and then with pure water in an ultrasonic bath (US-4R, AS-ONE, Japan) for 1 min each. The washed PTFE sheets were dried using  $N_2$  gas (99.99%, Iwatani Fine Gas, Japan).

### Heat-assisted plasma (HAP) treatment

The atmospheric-pressure plasma reactor (Meisyo Kiko, Japan) consisted of a high-frequency power supply ( $f = 13.56$  MHz, KD-01, Noda RF Technologies, Japan), a matcher, a chamber, an oil rotary vacuum pump (EC603, Ulvac, Japan), an electrode made of Cu pipe ( $L = 100$  mm,  $d = 1.8$  mm,  $\varnothing = 3$  mm) covered with an alumina pipe ( $L = 100$  mm,  $d = 3$  mm,  $\varnothing = 5$  mm), a screw for adjusting the distance between the electrode and the surface of the PTFE sheet, and a cylindrical rotating stage ( $L = 34$  mm,  $\varnothing = 40$  mm) for fixing the PTFE sheet. One side of the PTFE sheet was fixed to the rotating stage using polyimide double-sided tape (3M, Japan). The other side of the PTFE sheet was placed between two metal plates ( $L = 34$  mm,  $W = 11$  mm,  $t = 1.5$  mm, and  $L = 34$  mm,  $W = 0.8$  mm,  $t = 1.5$  mm) and fixed to the rotating stage with screws and a spring to keep it under tension. Before the plasma treatment, the pressure in the reactor was decreased using an oil rotary vacuum pump. At this time, the BP was adjusted to 1000, 9, or 5 Pa. He gas (99.99%, Iwatani Fine Gas, Japan) was then flowed into the reactor until it reached atmospheric pressure (101 300 Pa). The plasma treatment conditions are shown in Table 1. Plasma treatment at low temperature ( $<100$  °C) has previously been reported to have little effect on the adhesion properties of PTFE, whereas HAP treatment ( $>200$  °C) has been reported to strongly affect its adhesion properties. Two types of HAP treatments have been developed. The first method involves increasing the surface temperature naturally ( $>200$  °C) by increasing the input power density used to generate the plasma. The second approach is to raise the surface temperature ( $>200$  °C) using a halogen heater. A digital radiation thermometer (FT-H40K and FT-50A, Keyence,

Table 1 Plasma treatment conditions

Power frequency	13.56 MHz
Electrode-sample gap	1.0 mm
Base pressure (BP)	1000, 9, 5 Pa
Process gas	He
Input power	19.1 W cm <sup>-2</sup>
Scan speed	2 mm s <sup>-1</sup>
Number of round trips	60 times
Irradiation time	600 s (total 1800 min)



Japan) was used to measure the temperature of the PTFE surface during the HAP treatment. In this study, the former HAP treatment method was adopted and the surface modification resulting from a change in the BP was investigated.

### Residual oxygen concentration measurements

The value of etching rate during HAP treatment was determined by the amount of the residual oxygen concentration in the chamber. First, the chamber was evacuated to 1000, 9, 5 Pa, and filled with He gas up to atmospheric pressure. Then, the residual oxygen concentration in the chamber was measured using a zirconia-type oxygen analyzer (LC-300, Toray Engineering, Japan). To confirm the reproducibility, the residual oxygen concentration was measured three times under each of the same condition. The average residual oxygen concentration was defined as an arithmetic mean value, and the error bar was shown as a standard error.

### Etching-rate measurements

During the HAP treatment, the PTFE surface was etched and its sample's mass decreased. The mass loss was quantified by weighing the PTFE samples before and after the HAP treatment using a high-accuracy electronic balance (HR202i, A&D Company, Japan). The etching rate was calculated by dividing the average mass loss by the area of the plasma-treated surface (34 mm × 30 mm) and the total treatment time (1800 s) and was expressed in  $[\mu\text{g}(\text{cm}^2\text{ s})^{-1}]$ . Three samples were prepared under each of the same condition to confirm the reproducibility. The average etching rate was defined as an arithmetic mean value, and the error bar was shown as a standard error.

### Optical emission spectroscopy (OES)

Optical emission spectroscopy was used to identify the active species in the plasma treatment. The OES spectrum was measured using a fiber multichannel spectrometer (HR4000, Ocean Insight, Japan) in the range of 200 to 1000 nm and an optical fiber (P400-2-UV/VIS, Ocean Insight, Japan). The exposure time was 0.5 s.

### X-ray photoelectron spectroscopy (XPS)

The HAP treatment significantly changed the chemical composition of the PTFE surface. In this study, the chemical composition of the PTFE surface was investigated using an X-ray photoelectron spectrometer (Quantum-2000, ULVAC-PAI, Japan) equipped with an Al-K $\alpha$  source. The irradiation diameter was 100  $\mu\text{m}$ , the acceleration voltage was 15 kV, the pass energy was 23.50 eV, the step size was 0.05 eV, and the number of integration times was three. The binding energies of as-received and HAP-treated PTFE were adjusted so that the peak binding energies of CF<sub>2</sub> were 292.5 and 291.8 eV, respectively.<sup>16,32,35–38</sup> Each C 1s-XPS spectrum was deconvoluted into eight peaks (CF<sub>3</sub>, CF<sub>2</sub>, C–F, O–C=O, C=O, C–O, C–C, and C=C) using data analysis software (XPSPEAK Ver. 4.1, Free download). The peaks indexed to CF<sub>3</sub>, CF<sub>2</sub>, and C–F were then grouped as the fluorine group, the peaks indexed to O–C=O,

C=O, and C–O were grouped as the oxygen group, and the peaks indexed to C–C and C=C were grouped as the carbon group.

### Surface morphology observation using a scanning electron microscope (SEM)

Because the PTFE surface was etched by the HAP treatment, we expected the surface morphology to change. The surface morphology of the PTFE before and after HAP treatment was investigated using a scanning electron microscope (JCM-6000, JEOL, Japan). Before the observation, a thin Au film was applied to each sample using an ion-sputtering apparatus (Smart Coater DII-29010SCTR, JEOL, Japan) to prevent the electrification of the sample.

### Surface hardness test

The surface hardness is affected by the HAP treatment. Therefore, load–depth data were collected from 0 to 40  $\mu\text{N}$  at 20 ms intervals using a nanoindenter (ENT-2100, Elionix, Japan). The surface hardness was calculated by dividing the maximum load by the projected contact area. Surface hardness histograms were constructed by measuring the indentation hardness at 50 different points for each sample. The synergistic mean value obtained from the test results was defined as the surface hardness.

### Adhesion strength measurements

To evaluate the adhesion property, a two-component epoxy (EP) adhesive (epoxy resin AV-138 and hardener HV-998, Nagase Chemtex, Japan) and an unvulcanized isobutylene–isoprene rubber (IIR) sheet were used. Each was adhered to PTFE using the same method as described in previous studies.<sup>32,39</sup> The PTFE/EP-adhesive/SUS304 adhesion strength was measured *via* a 90° peel test using a digital force gauge (ZP-200N, Imada, Japan) and an electrically driven stand (MX-500N, Imada, Japan). The PTFE/IIR adhesion strength was measured *via* a T-peel test using the same digital force gauge and the electrically driven stand used in the 90° peel test. To confirm the reproducibility, three samples were prepared under each of the same condition. The average adhesion strength was defined as an arithmetic mean value, and the error bar was shown as a standard error.

## Results and discussion

### Effect of base pressure (BP) on macroscopic changes in PTFE

As previously aforementioned, the etching rate depends on the residual oxygen in the chamber. Therefore, we expected the etching rate to relatively decrease with a decrease in BP. Fig. 1(a) shows photographs of PTFE samples before and after HAP treatment at different BPs. The PTFE sheets HAP-treated at BP = 1000 Pa were thinned and made translucent by the HAP treatment. This result is attributed to excessive etching caused by too much residual O<sub>2</sub> in the chamber. In contrast, for the PTFE sheets HAP-treated at BPs = 9 and 5 Pa, visual observation did not change. Fig. 1(b) shows the residual oxygen concentration



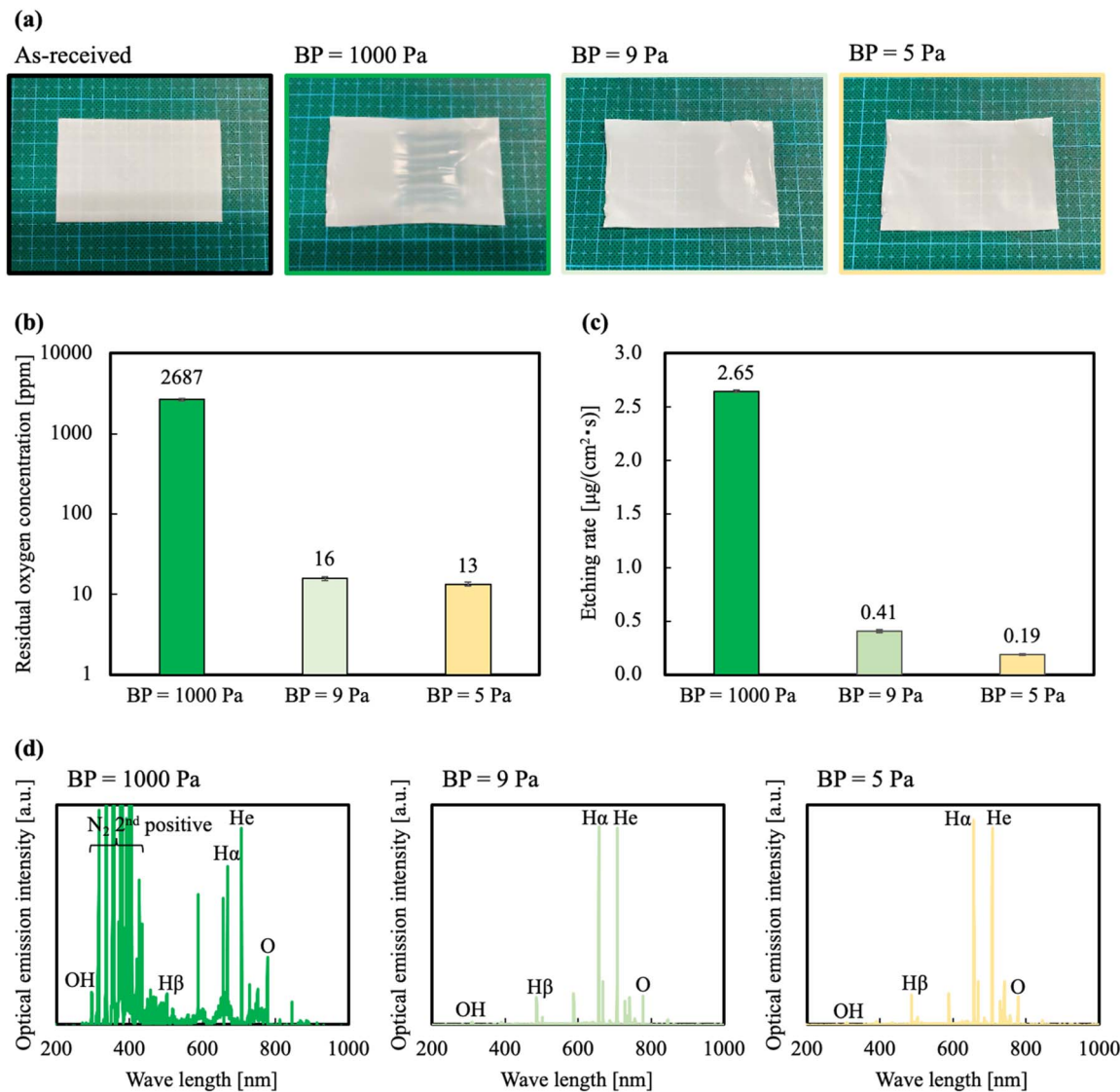


Fig. 1 (a) Photographs of the PTFE before and after HAP treatments at different BPs, (b) relation between residual oxygen concentration and BP, and (c) relation between etching rates of the HAP-treated PTFE and BP, and (d) OES spectra in HAP treatment at different BPs.

in the chamber when adjusted to each base pressure. At BPs = 1000, 9, and 5 Pa, the residual oxygen concentration was 2687, 16, and 13 ppm, respectively. Fig. 1(c) shows the calculation results of the etching rate when the HAP treatment was performed at different BPs. At BPs = 1000, 9, and 5 Pa, the etching rates were 2.65, 0.41, and 0.19  $\mu\text{g}/(\text{cm}^2 \cdot \text{s})^{-1}$ , respectively. The weights of the samples decreased at all of the investigated BPs, indicating that the PTFE surface was etched by the HAP treatment. Because of this comparison, the etching rate of the HAP treatment at BP = 1000 Pa was the largest among all of the investigated BPs and was 13.9 times greater than that of the HAP treatment at BP = 5 Pa. However, the etching rates of the HAP treatment at BPs = 9 and 5 Pa decreased by 15.5% and 7.2% compared with that of the HAP treatment at BP = 1000 Pa. Fig. 1(d) shows OES spectra of HAP treatments at different BPs. The emission intensities of the OH radical (309 nm) and the O radical (777 nm) decreased with a decrease in the BP. Comparing the emission intensity of the OH radical and the O

radical, the emission intensity of the O radical was higher. Therefore, we speculated that the O radical was the main factor for the etching. The emission intensity of the OH radical and O radical decreased with decreasing BP. For the PTFE sample HAP-treated at BP = 1000 Pa, the peaks at 330–400 nm were very strongly detected. These peaks show the emission of the second positive system bands of nitrogen. At BP = 1000 Pa, the effect of residual air was found to be compelling. For the PTFE sample HAP-treated at BP = 9 and 5 Pa, both were dominated by He emission. Next, we investigated whether the WBL was sufficiently removed and repaired and whether O-containing functional groups were introduced onto the PTFE surface.

#### Effect of base pressure (BP) on microscopic changes of PTFE surface

Because the etching rates of the HAP treatment at BPs = 9 and 5 Pa were low, we investigated the effect of BP on the surface



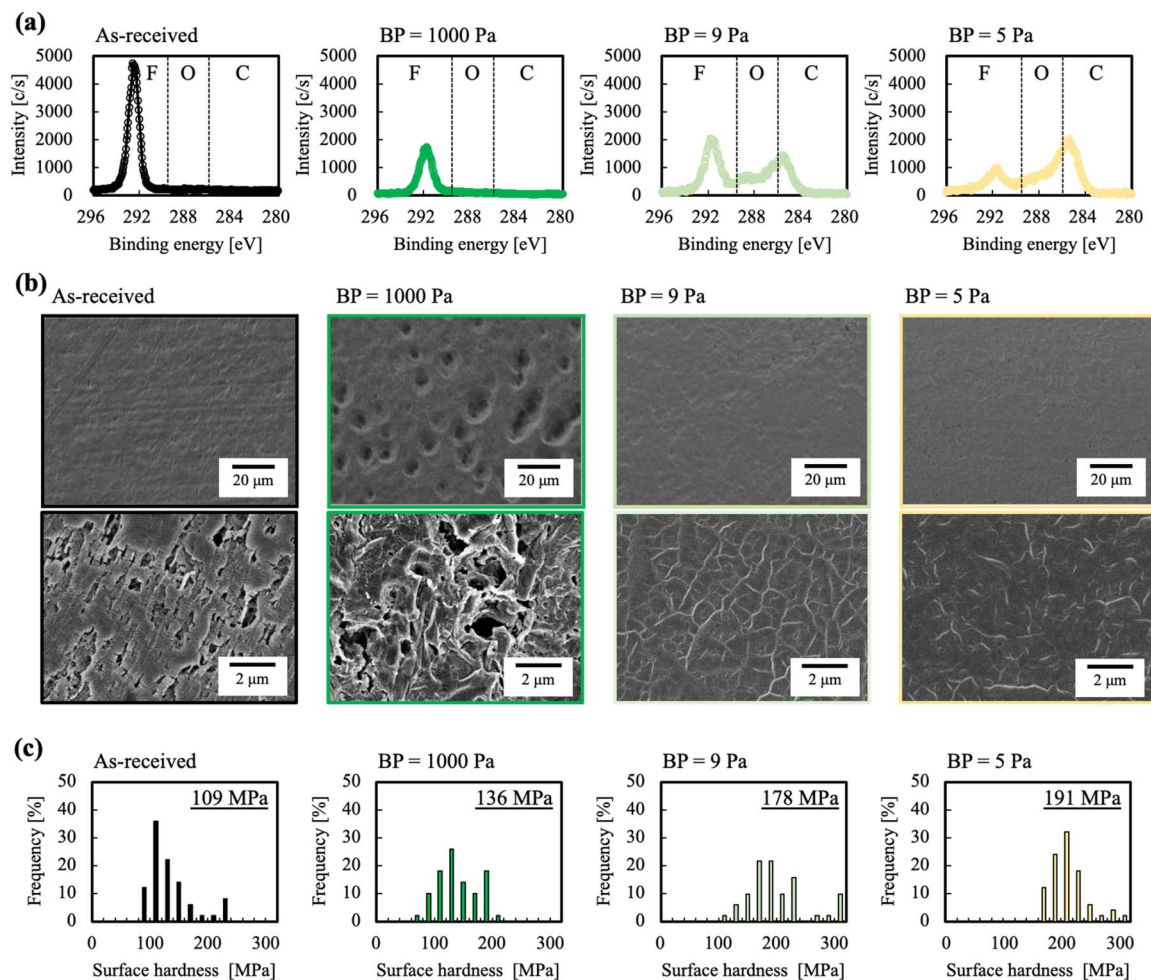


Fig. 2 (a) C 1s-XPS spectra of the PTFE surface before and after HAP treatment at different BPs, (b) SEM images of the PTFE surface before and after HAP treatment at different BPs, and (c) histograms of the surface hardness of the PTFE surface before and after HAP treatment at different BPs.

chemical composition of PTFE. The chemical composition of the PTFE surface HAP-treated at BPs = 1000, 9, and 5 Pa was investigated using X-ray photoelectron spectroscopy (XPS). Fig. 2(a) shows the C 1s-XPS spectra of the PTFE samples. Table 2 shows the group names and the ratios calculated from the peak resolution of the C 1s-XPS spectra. The method for calculating group ratios is shown in ESI-1 and 2.† For the PTFE sample HAP-treated at BP = 1000 Pa, peaks indexed to O-C=O, C=O, C-O, and C-C from the plasma-modified layer were not detected on the surface; similar results were obtained for the as-received PTFE. An excessively high etching rate leads to excessive etching; that is, if the plasma-modified layer was also etched, the PTFE surface would lack a plasma-modified layer.

For the PTFE sample HAP-treated at BP = 9 Pa, the intensity of the peak indexed to CF<sub>2</sub> decreased and the intensities of the peaks indexed to O-containing functional groups (e.g., O-C=O (289.2 eV), C=O (288.0 eV) and C-O (286.5 eV) as well as C-C (285.3 eV) crosslinkings) increased. Surprisingly, the shape of the C 1s-XPS spectra of the PTFE sample HAP-treated at BPs = 9 and 5 Pa appeared axisymmetric with respect to the Y-axis. In the C 1s-XPS spectrum of the PTFE sample HAP-treated at BP = 5 Pa, the intensity of the CF<sub>2</sub> peak substantially decreased and the intensities of the O-C=O, C=O, C-O, and C-C peaks increased compared with those in the spectrum of the as-received PTFE. When the BP was lowered from 1000 to 9 to 5 Pa, the fluorine-group ratio decreased from 100 to 47 to 25%,

Table 2 Group ratios of fluorine, oxygen, and carbon on the PTFE surface before and after HAP treatments at different BPs

Sample name	As-received	BP = 1000 Pa	BP = 9 Pa	BP = 5 Pa
Fluorine group [%] (CF <sub>3</sub> , CF <sub>2</sub> , C-F)	100	100	47	25
Oxygen group [%] (O-C=O, C=O, C-O)	0	0	26	35
Carbon group [%] (C-C, C=C)	0	0	27	40



the oxygen-group ratio increased from 0 to 26 to 35%, and the carbon-group ratio increased from 0 to 27 to 40%, respectively. In brief, we found that the ratio of the sum of oxygen and carbon groups derived from the plasma-modified layer increased from 0% for the as-received PTFE to a maximum of 75% for the HAP-treated PTFE samples. We speculated that the O-containing functional groups and C-C crosslinkings easily remained on the PTFE surface because the excessive etching was suppressed, resulting in a large change in the ratio of the sum of the oxygen and carbon groups. This result supports our hypothesis that excessive etching occurs and leads to etching of the plasma-modified layer when the BP is high.

For the PTFE samples HAP-treated at BPs = 9 and 5 Pa, whether sufficient removal of the WBL was achieved is difficult to determine from only the results of the surface chemical composition analysis. We therefore used scanning electron microscopy (SEM) to observe the surface morphology of the PTFE before and after the HAP treatment. Fig. 2(b) shows SEM images of the PTFE samples HAP-treated at different BPs. For the as-received PTFE, numerous linear cutting scratches are observed. These scratches are introduced during the manufacturing process and are a cause of WBL formation.<sup>6,7,40</sup> For the PTFE sample HAP-treated at BP = 1000 Pa, no linear cutting scratches are observed; however, large holes, as if the PTFE surface had been gouged, are observed across the entire sample. The amorphous component of the PTFE surface has been reported to be more susceptible to etching by atomic O than the crystalline component.<sup>41</sup> Therefore, we speculated that numerous holes were formed and the surface roughness increased because of this greater susceptibility to etching. For the PTFE samples HAP-treated at BPs = 9 and 5 Pa, the linear cutting scratches were not observed and surface planarization was confirmed. The PTFE surface was flattened because the low etching rate resulted in the removal of the linear cutting scratches without inducing excessive etching. No substantial differences were observed in the SEM image of the PTFE sample

HAP-treated at BP = 9 Pa and that of the sample treated at BP = 5 Pa. From these results, we concluded that, even if the etching rate is decreased to some extent, the WBL can be sufficiently removed.

If the WBL on the PTFE surface is removed and/or the C-C crosslinkings are formed by the HAP treatment, the surface hardness of PTFE will inevitably increase. The surface hardness of the PTFE before and after HAP treatment was therefore investigated using a nanoindenter. The representative load-depth curve is shown in ESI-3.† Fig. 2(c) shows histograms of the surface hardness of the PTFE samples HAP-treated at different BPs. The as-received PTFE sample exhibited the lowest surface hardness (108 MPa). The surface hardness of all the HAP-treated PTFE samples was greater than that of the as-received PTFE sample. These results indicate that the WBL of the PTFE surface was etched and removed by the HAP treatment, exposing a new surface from the bulk. Additionally, the surface hardness of the HAP-treated PTFE sample decreased with increasing BP. The decreasing surface hardness is attributed to the decrease of C-C crosslinkings formed by the HAP treatment; the PTFE samples are probably etched by a HAP treatment at a higher BP. The PTFE sample HAP-treated at BP = 5 Pa exhibited the highest surface hardness (191 MPa). Among the XPS results, the peaks indexed to C-C crosslinking were most intense in the spectrum of the PTFE sample HAP-treated at BP = 5 Pa. Additionally, the removal of the WBL on the PTFE surface was confirmed from the SEM images. In summary, the surface hardness results are consistent with the results of the XPS and SEM analyses.

### Effect of base pressure (BP) on adhesion properties

To compare the adhesion properties of PTFE in the presence or absence of an adhesive, an epoxy (EP) adhesive and an unvulcanized isobutylene-isoprene rubber (IIR) sheet were used. Fig. 3(a) shows the PTFE/EP-adhesive/SUS304 adhesion

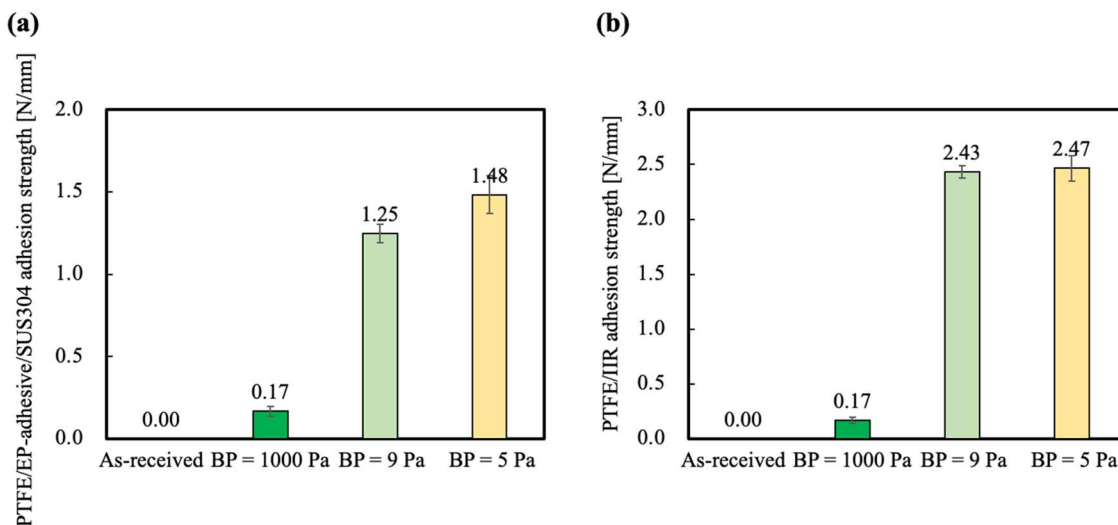


Fig. 3 Adhesion properties of PTFE before and after HAP treatment at different BPs: (a) PTFE/EP-adhesive/SUS304 adhesion strengths, (b) PTFE/IIR adhesion strengths.

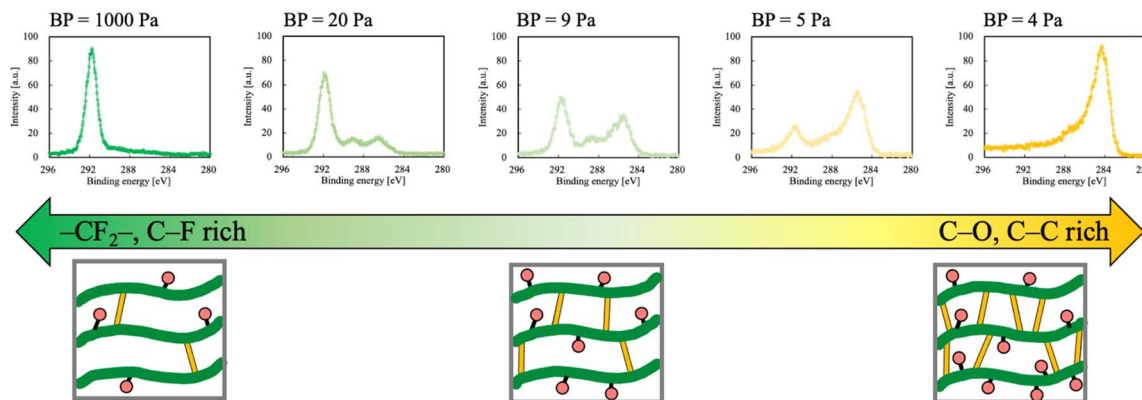


Fig. 4 Flexible selection of functional group ratio *via* HAP treatment with BP control: green tube, red round and yellow bar indicate  $\text{CF}_2$  main chains, O-containing functional groups, and C–C crosslinkings, respectively.

strengths of the PTFE samples HAP-treated at different BPs. The PTFE/EP-adhesive/SUS304 adhesion strength of the as-received PTFE sample was  $0.0 \text{ N mm}^{-1}$ . The PTFE/EP-adhesive/SUS304 adhesion strength of the PTFE sample HAP-treated at BP = 1000 Pa was  $0.17 \text{ N mm}^{-1}$ , which is greater than that of the as-received PTFE but not sufficient for practical use. By contrast, the PTFE/EP-adhesive/SUS304 adhesion strengths of the PTFE HAP-treated at BPs = 9 and 5 Pa are greater than  $1.0 \text{ N mm}^{-1}$ , which indicates a substantial improvement in the adhesion strength of PTFE. A negative correlation was observed between the BP and the PTFE/EP-adhesive/SUS304 adhesion strength.

Fig. 3(b) shows the PTFE/IIR adhesion strengths of the PTFE samples HAP-treated at different BPs. The PTFE/IIR adhesion strength of the as-received PTFE sample was also  $0.0 \text{ N mm}^{-1}$ . The PTFE/IIR adhesion strength of the PTFE sample HAP-treated at BP = 1000 Pa was  $0.17 \text{ N mm}^{-1}$ , which is greater than that of the as-received PTFE but, like the PTFE/EP-adhesive/SUS304 adhesion strength of PTFE HAP-treated at BP = 1000 Pa, not sufficient for the material to be used in practical applications. The PTFE/IIR adhesion strengths of the PTFE samples HAP-treated at BPs = 9 and 5 Pa were greater than  $2.0 \text{ N mm}^{-1}$ , and cohesion failure of IIR occurred during the T-peel test. Unfortunately, we could not compare the adhesion strengths of the PTFE samples HAP-treated at BPs = 9 and 5 Pa because the IIR caused cohesion failure. XPS analysis confirmed that a large number of O-containing functional groups and C–C crosslinkings from the plasma-modified layer remained when the etching rate decreased with a decrease in BP. Therefore, the results of XPS analysis and adhesion strength tests indicate that suppressing the etching of the plasma-modified layer enhanced the adhesion properties of the PTFE.

### Control of the functional-group ratio

Fig. 4 shows the surface-controlled PTFE of the functional-group ratios *via* HAP treatment with different BPs before plasma treatment. When the plasma treatment condition had high BP, the fluorine group ratio was high because He plasma contained a high oxygen concentration then the etching rate also increased. When the ratio of the fluorine group decreased

with decreasing the BP, the ratios of the oxygen and carbon groups increased because He plasma contained a low oxygen concentration then the etching rate also decreased. Especially, when the plasma treatment condition had the lowest BP = 4, the peak of the fluorine group vanished in spite of a fluoropolymer surface and the peaks of the oxygen and carbon groups were detected. The plasma-treated PTFE surface with no peak of the fluorine group resembles a PTFE surface treated *via* chemical etching using Na–naphthalene or Na–ammonium complex solution. This result indicates that plasma treatment with BP control enables flexible selection of the functional-group ratio on a PTFE surface and replacement from chemical etching to plasma treatment, which would result in environmental loading reduction.

## Conclusions

We hypothesized that controlling the etching rate of PTFE by lowering the BP would inhibit excessive etching of the PTFE surface and control the ratio of functional groups even when a single gas is used. Therefore, in this study, we investigated the effect of the BP on the etching rate, surface chemical composition, surface morphology, surface hardness, and the adhesion properties of PTFE. The etching rate decreased with decreasing BP. We confirmed that controlling the BP enabled control of the etching rate. In the XPS spectra, the intensity of peaks associated with  $\text{CF}_2$  on the PTFE surface decreased and the intensities of peaks associated with O-containing functional groups and C–C crosslinkings increased with a decrease in BP. SEM observations revealed that the PTFE surface was planarized at low BPs. The surface hardness results confirmed that the surface hardness increased with decreasing BP. The adhesion strength results confirmed that the adhesion strength also increased with decreasing BP. The PTFE/IIR adhesion strengths of the PTFE samples HAP-treated at BPs = 9 and 5 Pa were greater than  $2 \text{ N mm}^{-1}$ , and the cohesion failure of IIR occurred during the T-peel tests.

These results demonstrate that our hypothesis was correct. In short, controlling the etching rate by manipulating the BP prevented excessive etching of the PTFE surface and enabled the



ratio of functional groups to be controlled even when a single gas was used. These results indicate that the PTFE surface state can be freely determined. In applications where the high-frequency characteristics of PTFE are important such as substrate materials for printed circuit boards, the PTFE surface with a high ratio of  $\text{CF}_2$  can be controlled, whereas in applications where the adhesion properties of PTFE are important such as sliding materials strongly adhered to structural steel for base isolation, a PTFE surface with a high ratio of O-containing functional groups and C–C crosslinkings can be prepared. Thus, the PTFE surface can be rendered suitable for various applications. Only one parameter (BP) was used to control the plasma characteristics. Because the WBL can be completely removed if the etching rate is further decreased, the selection of the optimal BP is important.

## Author contributions

Yuji Ohkubo: validation, formal analysis, investigation, writing – review & editing, project administration. Yuki Okazaki: validation, formal analysis, investigation, writing – original draft. Misa Nishino: formal analysis, investigation. Yosuke Seto: formal analysis, investigation. Katsuyoshi Endo: discussion, supervision. Kazuya Yamamura: discussion, supervision.

## Conflicts of interest

The authors declare no conflict of interest.

## Acknowledgements

The IIR was provided gratis by Hyogo Prefectural Institute of Technology; we thank them for their assistance. The graphical abstract partially contains illustrations downloaded from iStock that is free illustration download system; we thank the illustrators, the free download system, and the company ACworks Co. Ltd.

## References

- 1 Z. Bin Li, H. Y. Li, Y. J. Fan, L. Liu, Y. H. Chen, C. Zhang and G. Zhu, *ACS Appl. Mater. Interfaces*, 2019, **11**, 20370–20377.
- 2 T.-L. Chen, C.-Y. Huang, Y.-T. Xie, Y.-Y. Chiang, Y.-M. Chen and H.-Y. Hsueh, *ACS Appl. Mater. Interfaces*, 2019, **11**, 40875–40885.
- 3 L. J. Bannenberg, B. Boshuizen, F. A. Ardy Nugroho and H. Schreuders, *ACS Appl. Mater. Interfaces*, 2021, **13**, 52530–52541.
- 4 H. Schonhorn and R. H. Hansen, *J. Appl. Polym. Sci.*, 1967, **11**, 1461–1474.
- 5 J. J. Bikerman, *Ind. Eng. Chem.*, 1967, **59**, 40–44.
- 6 D. M. Brewis, I. Mathieson, I. Sutherland and R. A. Cayless, *J. Adhes.*, 1993, **41**, 113–128.
- 7 D. M. Brewis, *Int. J. Adhes. Adhes.*, 1993, **13**, 251–256.
- 8 M. L. Miller, R. H. Postal, P. N. Sawyer, J. G. Martin and M. J. Kaplit, *J. Appl. Polym. Sci.*, 1970, **14**, 257–266.
- 9 D. W. Dwight and W. M. Riggs, *J. Colloid Interface Sci.*, 1974, **47**, 650–660.
- 10 J. T. Marchesi, H. D. Keith and A. Garton, *J. Adhes.*, 1992, **39**, 185–205.
- 11 I. Mathieson, D. M. Brewis, I. Sutherland and R. A. Cayless, *J. Adhes.*, 1994, **46**, 49–56.
- 12 M. Gabriel, M. Dahm and C.-F. Vahl, *Biomed. Mater.*, 2011, **6**, 035007.
- 13 M. E. Ryan and J. P. S. Badyal, *Macromolecules*, 1995, **28**, 1377–1382.
- 14 G. Borgia, A. Chiper and I. Rusu, *Plasma Sources Sci. Technol.*, 2006, **15**, 849–857.
- 15 J. Hubert, T. Dufour, N. Vandencastele, S. Desbief, R. Lazzaroni and F. Reniers, *Langmuir*, 2012, **28**, 9466–9474.
- 16 Y. Momose, Y. Tamura, M. Ogino, S. Okazaki and M. Hirayama, *J. Vac. Sci. Technol., A*, 1992, **10**, 229–238.
- 17 E. A. D. Carbone, N. Boucher, M. Sferrazza and F. Reniers, *Surf. Interface Anal.*, 2010, **42**, 1014–1018.
- 18 M. Kiruthika, K. Nivetha and G. Shanmugavelayutham, *Mater. Res. Express*, 2019, **6**, 115350.
- 19 R. Zaplotnik and A. Vesel, *Polymers*, 2020, **12**, 1136.
- 20 J. C. Caro, U. Lappan and K. Lunkwitz, *Surf. Coat. Technol.*, 1999, **116–119**, 792–795.
- 21 D. Lojen, R. Zaplotnik, G. Primc, M. Mozetič and A. Vesel, *Appl. Surf. Sci.*, 2020, **533**, 147356.
- 22 A. Vesel, J. Kovac, R. Zaplotnik, M. Modic and M. Mozetic, *Appl. Surf. Sci.*, 2015, **357**, 1325–1332.
- 23 U. Lappan, H.-M. Buchhammer and K. Lunkwitz, *Polymer*, 1999, **40**, 4087–4091.
- 24 D. D. Pappas, A. A. Bujanda, J. A. Orlicki and R. E. Jensen, *Surf. Coat. Technol.*, 2008, **203**, 830–834.
- 25 C. Sarra-Bournet, S. Turgeon, D. Mantovani and G. Laroche, *J. Phys. D: Appl. Phys.*, 2006, **39**, 3461–3469.
- 26 C. Sarra-Bournet, G. Ayotte, S. Turgeon, F. Massines and G. Laroche, *Langmuir*, 2009, **25**, 9432–9440.
- 27 J. R. Hollahan, B. B. Stafford, R. D. Falb and S. T. Payne, *J. Appl. Polym. Sci.*, 1969, **13**, 807–816.
- 28 M. Okubo, M. Tahara, Y. Aburatani, T. Kuroki and T. Hibino, *IEEE Trans. Ind. Appl.*, 2010, **46**, 1715–1721.
- 29 T. Kuroki, M. Tahara, T. Kuwahara and M. Okubo, *IEEE Trans. Ind. Appl.*, 2014, **50**, 45–50.
- 30 M. Okubo, T. Onji, T. Kuroki, H. Nakano, E. Yao and M. Tahara, *Plasma Chem. Plasma Process.*, 2016, **36**, 1431–1448.
- 31 W. Hai, T. Hi, K. Shimizu and T. Yajima, *J. Photopolym. Sci. Technol.*, 2015, **28**, 479–483.
- 32 Y. Ohkubo, K. Ishihara, H. Sato, M. Shibahara, A. Nagatani, K. Honda, K. Endo and Y. Yamamura, *RSC Adv.*, 2017, **7**, 6432–6438.
- 33 N. Inagaki, S. Tasaka and T. Umehara, *J. Appl. Polym. Sci.*, 1999, **71**, 2191–2200.
- 34 G. Primc, *Polymers*, 2020, **12**, 2295.
- 35 Y. Ohkubo, T. Nakagawa, K. Endo and K. Yamamura, *RSC Adv.*, 2019, **9**, 22900–22906.
- 36 D. J. Wilson, R. L. Williams and R. C. Pond, *Surf. Interface Anal.*, 2001, **31**, 385–396.





- 37 N. Vandecasteele and F. Reniers, *J. Electron Spectrosc. Relat. Phenom.*, 2010, **178–179**, 394–408.
- 38 J. Hubert, T. Dufour, N. Vandecasteele, S. Desbief, R. Lazzaroni and F. Reniers, *Langmuir*, 2012, **28**, 9466–9474.
- 39 Y. Ohkubo, M. Shibahara, A. Nagatani, K. Honda, K. Endo and K. Yamamura, *J. Adhes.*, 2020, **96**, 776–796.
- 40 Y. Seto, M. Nishino, Y. Okazaki, K. Endo, K. Yamamura and Y. Ohkubo, *Polym. J.*, 2022, **54**, 79–81.
- 41 J. Hubert, J. Mertens, T. Dufour, N. Vandecasteele, F. Reniers, P. Viville, R. Lazzaroni, M. Raes and H. Terryn, *J. Mater. Res.*, 2015, **30**, 3177–3191.

